

Acoustical properties of irregular and fractal cavities

B. Sapoval, O. Haeberlé, and S. Russ

Laboratoire de Physique de la Matière Condensée, Ecole Polytechnique, C.N.R.S., 91128 Palaiseau Cédex, France

(Received 4 December 1996; accepted for publication 23 May 1997)

Acoustical properties of irregular cavities described by fractal shapes are investigated numerically. Geometrical irregularity has three effects. First, the low-frequency modal density is enhanced. Second, many of the modes are found to be localized at the cavity boundary. Third, the acoustical losses, computed in a boundary layer approximation, are increased proportionally to the perimeter area of the resonator and a mathematical fractal cavity should be infinitely damped. We show that localization contributes to increase the losses. The same considerations should apply to acoustical waveguides with irregular cross section. © 1997 Acoustical Society of America.

[S0001-4966(97)00210-5]

PACS numbers: 43.20.Ks [ANN]

INTRODUCTION

Geometrical irregularities appear in many natural and artificial systems and their vibrational properties are of general interest. How trees respond to wind, and how sea waves depend on the topography or geometrical structure of the coasts and breakwaters are largely unanswered questions. The emergence of fractal geometry has been a significant breakthrough in the description of strong geometrical irregularity and its associated physical properties.^{1,2} The fractal language permits discussion of this question in a well-defined and documented geometrical framework. Not only does fractal geometry permit a description of strong statistical irregularity, but it also allows consideration of the deterministic fractals as simple models for extreme geometrical disorder. When the physical properties of the objects that we consider are due to the hierarchical character of their geometry, then their physical properties can be studied on deterministic fractal objects.² This is, for example, the case for self-similar electrodes where the study of deterministic systems is readily applicable to random self-similar structures.³

The three main properties of resonators are their spectrum or modal distribution, the spatial distribution of the modes (which may exhibit localization or confinement effects), and their damping. Current empirical knowledge about waves and resonators indicates that a perturbation of a resonator geometry may strongly modify the quality factor of resonances. It has already been shown in the case of “mass fractals” vibrations (the so-called fractons modes) that geometrical irregularity has a strong effect on damping.⁴

We address here the same general question for acoustical cavities: Do the geometrical irregularities play a role in the losses and why? We believe that the study of fractal resonators can help to understand the acoustical properties of irregular cavities in general, with possible application to room acoustics, acoustical waveguides, and anechoic chambers. The problem of the asymptotic (high-frequency) density of states in fractal resonators has already been studied from a mathematical point of view.⁵⁻⁹

Experimental observation and numerical investigation of the low-frequency vibrations of fractal drums are reported in

Refs. 10 and 11. The drum geometries were generated by iterative transformation of a square initiator, as shown in Fig. 1. The figure shows the contour of prefractals at generation $\nu=0$, $\nu=1$, and $\nu=2$. Systems in which the perimeter is only fractal, like a fractal drum or a fractal cavity, are called “surface fractals” and their vibrations are called “fractinos.” In the case of the fractal drum, the vibrations obey the Dirichlet boundary condition and are named Dirichlet fractinos.^{10,11}

Eigenmodes of 2-D prefractal resonators using Neuman boundary conditions, i.e., Neumann fractinos, have also been studied recently.^{12,13} This renders possible the study of acoustic modal density and damping in the 3-D prefractal cavities shown in Fig. 1. This is the purpose of the present work.

We show on two specific examples that the low-frequency modal distribution is strongly modified and that the damping is increased by a factor which depends of the degree of irregularity of the boundary. We also show that the localization effects found by Russ *et al.* contribute even more to increase the damping. The losses are computed from the spatial distribution of the modes as we recall below.

I. QUALITY FACTOR AND AMPLITUDE DISTRIBUTION

The quality factor Q_N of a resonator for a mode N is the ratio of the stored energy to the losses per cycle W_N

$$Q_N = 2\pi E_N / W_N. \quad (1)$$

The quality factor characterizes the ability of the resonator to accumulate reactive energy for a given power input. It also determines the life time $Q_N \omega_N^{-1}$ of the oscillation when no power source is present.

In this work we restrict to linear acoustics and consider the limit of “very” weak losses so that the amplitude distribution is well-approximated by the zero-loss cavity modes.¹⁴⁻¹⁶ We consider an eigenmode N at frequency ω_N with a pressure distribution:

$$p_N(x, y, z, t) = p_0 V^{1/2} \Psi_N(x, y, z) \cos(\omega_N t). \quad (2)$$

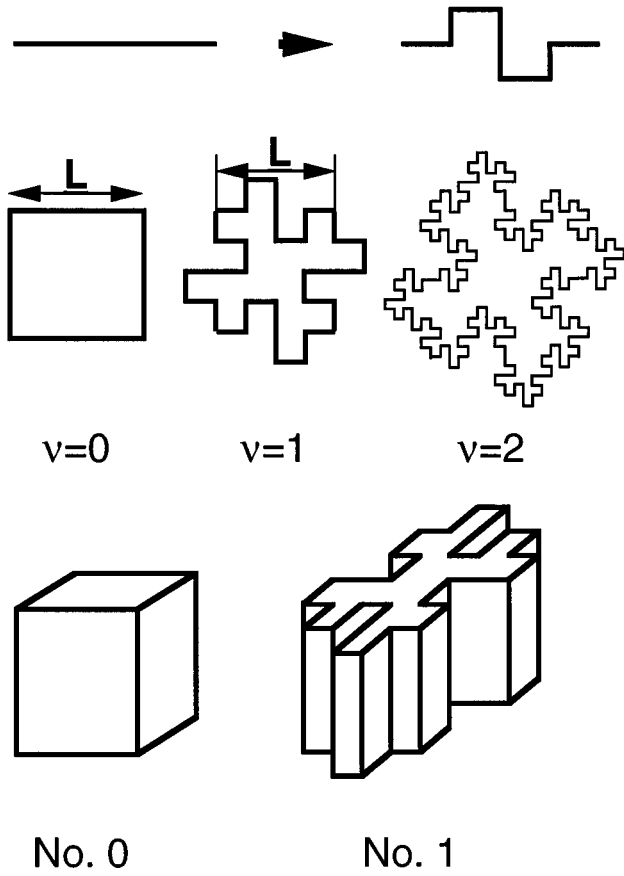


FIG. 1. System geometry. Top: Generator of the fractal geometry. Middle: Cross sections of the prefractal cavities under study. The area is conserved through the iteration process. Bottom: prefractal cavities of generation 0 (cubic cavity) and 1.

Here p_0 is the peak acoustic pressure and V is the volume of the cavity. Calling c the sound velocity, the pressure obeys the Helmholtz equation $\Delta P = (1/c^2)\partial^2 P/\partial t^2$ with the Neumann boundary conditions $\partial P/\partial n = 0$. This condition corresponds to a perfectly reflecting surface with no phase change. Eigenmodes $\Psi_N(x, y, z)$ satisfy the eigenvalue equation $\Delta \Psi_N = -(\omega_N^2/c^2)\Psi_N$. We normalize $\Psi_N(x, y, z)$ in the volume V by

$$\int \int \int_V dv \Psi_N^2(x, y, z) = 1. \quad (3)$$

The maximum elastic energy or kinetic energy is

$$E_N = p_0^2 V \int \int \int_V dv (c^2 \rho)^{-1} \Psi_N^2(x, y, z) = V p_0^2 / c^2 \rho, \quad (4)$$

where ρ is the density of the gas.

Acoustical losses in a rigid cavity are due to heat conduction and viscous dissipation. In the bulk, these losses are small at audio frequencies and are neglected here.¹⁴⁻¹⁶ Energy dissipation takes place at the cavity walls on a small boundary layer with a thickness of order 10^{-4} cm.^{15,17} To calculate the losses, it is convenient to replace the rigid walls by walls with a small admittance and to consider that there are no losses in the fluid. We are restricted here to prefractals in which the smaller flat element (smaller geometrical cutoff) is larger than this thickness.¹⁸ Our goal is to identify the

influence of the geometrical irregularity; we consider that our walls present a small but finite specific admittance $\epsilon(\omega)$. This admittance could be that of the real fluid boundary layer, or more simply, the admittance of a suitable sound absorbing material of small thickness covering the lateral cavity walls.

The energy dissipation is the total outflow of energy from the boundary. In the case of weak losses, the power L_N dissipated at the cavity boundaries can be expressed as a function of the zero-loss amplitude distribution by

$$L_N = V(p_0^2/\rho c) \int \int_S ds |\Psi_N^2(x, y, z)| \text{Re } \epsilon(\omega_N). \quad (5)$$

The quality factor of the mode N is given by

$$1/Q_N = [\text{Re } \epsilon(\omega_N)](c/\omega_N) \int \int_S ds |\Psi_N^2(x, y, z)|. \quad (6)$$

It can then be written $Q_N = 2\pi(\Lambda_N/\lambda_N)/[\text{Re } \epsilon(\omega_N)]$, where λ_N is the wavelength and

$$1/\Lambda_N = \int \int_S ds |\Psi_N^2(x, y, z)|. \quad (7)$$

Then, the higher the amplitude on the boundary, the lower the value of the length Λ_N and the lower the quality factor. Because our purpose is to study the dependence of the damping on the geometry, we have to know the amplitude distribution to compute this integral. This paper is organized as follows: We first recall briefly the numerical method.^{4,12} We then discuss the low-frequency modal density, the localization effects, and finally the effect of geometry on damping.

II. SOLUTION OF HELMHOLTZ EQUATION

As we work on cylindrical cavities with constant irregular cross sections, the variable z can be separated and the eigenfunctions takes the form

$$\Psi_N(x, y, z) = (2/L_z)^{1/2} \cos(m\pi z/L_z) \Psi_n(x, y), \quad (8)$$

with $m=0, 1, 2, \dots$ [for $m=0$, $\Psi_n(x, y, z) = L_z^{-1/2} \Psi_n(x, y)$]. The function $\Psi_n(x, y)$ satisfies the two-dimensional eigenvalue equation $\Delta \Psi_n = -(\omega_n^2/c^2)\Psi_n$ and is normalized over the cross section. The eigenfrequencies ω_N are given by

$$\omega_N^2 = \omega_n^2 + (m\pi c/L_z)^2. \quad (9)$$

Our numerical method to compute $\Psi_n(x, y)$ and ω_n^2 is to consider, instead of the Helmholtz equation, the time-dependent Fourier or diffusion equation:

$$D\Delta\Psi = \partial\Psi/\partial t. \quad (10)$$

In the Helmholtz equation, the variable is the acoustical pressure, i.e., a positive or negative departure for the normal fluid pressure. In Eq. (10), Ψ represents a concentration of diffusing particles, or a departure to a constant concentration, which in our case can also be either positive or negative. Equivalently, Eq. (10) is the Fourier heat equation and the

variable Ψ could represent positive or negative variations of the temperature around a constant value.

The general time-dependent solution of this equation is a combination of *real* exponentials of the form $\Psi = \sum_n c_n \Psi_n(x,y) \exp(-t/\tau_n)$, where τ_n satisfies an equivalent eigenvalue equation $\Delta \Psi_n = -(D\tau_n)^{-1} \Psi_n$ with the same boundary condition. In the diffusional approach, the Neumann boundary condition $\partial\Psi/\partial n=0$ means that diffusing particles are reflected at the boundary so there exists no net flux across the surface. Here it corresponds to the fact that the gas velocity is null on the walls.

The method is then to numerically compute the time-dependent solution of Eq. (10): Starting with an arbitrary initial function $z_0(x,y,t=0)$ the system will converge naturally to a function proportional to $\exp(-t/\tau_0)\Psi_0(x,y)$ yielding the first eigenstate $\Psi_0(x,y)$, the first eigenvalue $1/\tau_0$, and ω_0 through the correspondence $\omega_0^2/c^2=1/D\tau_0$. To compute the next state, one starts with a new trial function which is orthogonal to $\Psi_0(x,y)$. This new distribution converges with a time constant τ_1 to the next eigenfunction with non-zero initial weight, namely $\Psi_1(x,y)$. The procedure is then iterated and the states are obtained sequentially, by orthogonalization of the $(n+1)$ th initial distribution to the n previously computed eigenfunctions, thus converging to the $(n+1)$ th mode. The numerical implementation uses a finite difference method on a discretized system. It is discussed in detail in Refs. 4 and 12. One can find in these papers a discussion of the effects of the finite mesh size, of the convergence problems, and of roundoff errors on final precision.

III. MODAL DENSITY AND LEVEL SPACING

Two quantities play a dominant role in resonators studies: the density of states or modal density and the level spacing.¹⁴⁻¹⁶ Here we deal with the cavities obtained by ‘‘fractalization’’ of the cross section of a cube with side L .

The computation of the low-frequency modes for the 2-D systems shown in Fig. 1 is presented in Ref. 12. To obtain the eigenvalues ω_N^2 of the 3-D cavity, we have to combine the 2-D values ω_n^2 with the vertical modes using Eq. (9). We call $\omega_{n,\max}^2$ the largest eigenvalue that we have computed for a 2-D system. Some combinations of ω_n^2 with $(m\pi c/L_z)^2$ can give $\omega_N^2 \geq \omega_{n,\max}^2$. The 3-D modal density can therefore be exactly computed only for $\omega_N^2 \leq \omega_{n,\max}^2$. With 234, 240, and 214 computed states for systems 0, 1, and 2, we obtain, respectively, the first 2652, 2704, and 2329 modes of the corresponding cavities.

The vibrating modes of a cube of side L are labeled by the number $\mu, \mu',$ and μ'' of half-wavelengths in the x, y, z directions [with $\mu, \mu', \mu''=0,1,2,\dots$, and eigenvalues $\omega_{\mu,\mu',\mu''}^2=(\pi^2 c^2/L^2)(\mu^2+\mu'^2+\mu''^2)$]. We use in the following a reduced frequency $\Omega_N=\Omega_{n,m}=\omega_{n,m}/\omega_{1,0,0}$, where $\omega_{1,0,0}=\pi c/L$ is the fundamental frequency of the cubic cavity. For the cube we then have $\Omega_{\mu,\mu',\mu''}^2=(\mu^2+\mu'^2+\mu''^2)$.

The numerical results for the integrated modal density for the three cavities (with the same volume L^3) are shown in Fig. 2. They are to be compared with the high-frequency

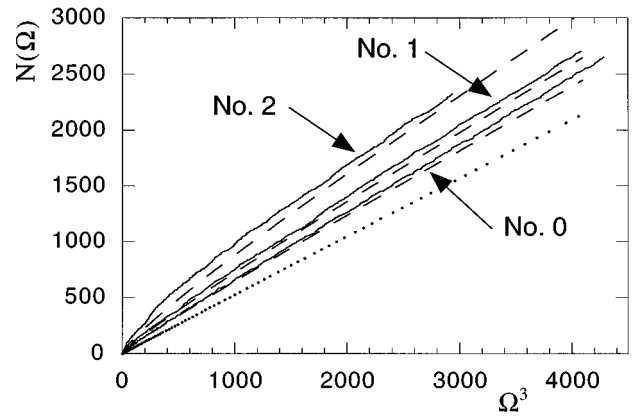


FIG. 2. Integrated modal density for cavities 0, 1, and 2. The dotted line represents the Weyl leading term. Dashed lines represent the Weyl approximation of Eq. (11).

Weyl approximation $N(\omega)=(1/6\pi^2)V(\omega/c)^3+(1/16\pi)\times S(\omega/c)^2$, which writes, with our reduced frequency units, as

$$N(\Omega)=(\pi/6)\Omega^3+(\pi/16)(S/L^2)\Omega^2, \quad (11)$$

where S is the total area of the cavity.¹⁹ For cavities 0, 1, and 2 the value of S is, respectively, equal to $6L^2, 10L^2,$ and $18L^2$.

In Fig. 2 the dotted line represents the Weyl leading term $(\pi/6)\Omega^3$ and the dashed lines represent Eq. (11) for the three cavities. The low-frequency modal density is notably increased by the irregularity. The high-frequency Weyl approximation still gives a good estimation of the modal density. Besides the net increase of the modal density due to increased fractalization one observes oscillations.^{9,12,13} These oscillations are due to the existence of a number of degenerate or quasi-degenerate states in our particular deterministic 2-D systems as explained in Ref. 12. These oscillations should not exist in irregular cavities where the feature sizes along the frontier are different or random.

The level spacing is modified in two ways. First, the increase in the modal density reduces the level spacing. Second, as discussed in Ref. 12, the pseudo-chaotic behavior of the 2-D systems induces a partial level repulsion. (This effect could be partially smeared out in 3-D.) These two facts should be reinforced by an increased irregularity.

IV. LOSSES IN PREFRACTAL CAVITIES

In order to selectively study the influence of the geometry on the losses, we consider in the following that the lower and upper surfaces of the cavities have infinite impedance. The losses are then restricted to the lateral surfaces.

Two different situations occur, depending on the nature of the modes, whether trivial modes or higher-order modes. For the trivial modes which correspond to the state $n=0$ of the 2-D problem for which $\Psi_{n=0}(x,y)=1/L$, integral (7) increases proportionally to the perimeter. These modes are then damped proportionally to the length of the perimeter of an horizontal cross section. Then a prefractal of generation ν presents losses which are 2^ν times larger than the cubic cavity, at least for the lower fractal generations. In our simpli-

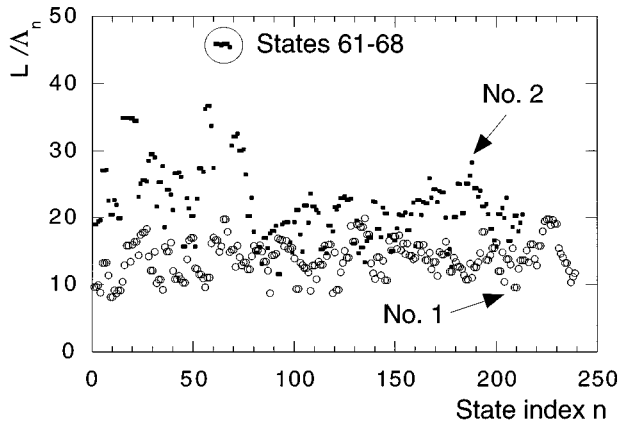


FIG. 3. Power dissipation, as measured by L/Λ_n , for the modes with $m=0$ of the three cavities in a boundary layer approximation. The dissipation is roughly proportional to the length of the perimeter. Some modes exhibit very high losses. For a cubic cavity, the losses take two different values. If $\mu=0, \mu' \neq 0$ (or $\mu \neq 0, \mu' = 0$), $L/\Lambda_n=6$. If $\mu \neq 0, \mu' \neq 0$, $L/\Lambda_n=8$.

fied framework a mathematical fractal would present infinite losses for all these modes as far as our model for the damping still holds. Although somewhat trivial, this statement is important and confirms the influence of fractal geometry on damping. Really, for high enough generation, the smaller cutoff would become smaller than the boundary layer and the problem has to be reconsidered.

More interesting are the higher-order modes ($n \neq 0$) which are of two types: those with $m=0$ and those with $m \neq 0$. If $m=0$ the integral in Eq. (7) factorizes as $ds=Ldl$, where dl is the differential element along the perimeter of a horizontal cross section of the cavity. For these modes the integral for the losses takes the form

$$1/\Lambda_n = \int_{\text{perimeter}} dl |\Psi_n^2(x,y)|. \quad (12)$$

If $m \neq 0$, the integral in Eq. (7) factorizes as $ds=(L/2)dl$ and the losses are simply smaller by a factor of 2 than those obtained from Eq. (12). The integral in Eq. (12) is the quantity that we actually compute from the knowledge of the amplitude distribution of the 2-D Neumann fractinos.

The results are shown in Fig. 3. For prefractal cavities the results indicate that the power dissipation [for constant $\epsilon(\omega)$] is increased by the irregularity of the frontier in a manner which is roughly proportional to the length of the perimeter, *as for the trivial modes*. For a few states, the prefractal systems exhibit still higher losses; for example, see states 61–68 of cavity No. 2. The higher losses for these particular states are due, as shown below, to the localization of these states in small regions near the cavity walls.

V. RELATION BETWEEN LOCALIZATION AND LOSSES

In this section we discuss why the confinement of a vibration in a restricted part of the cavity near the boundary increases the damping. The localization characterizes the irregular distribution of the vibration amplitude and was studied in Ref. 12. It was found that a number of modes were confined at the boundary, the amplitude the inner part of the

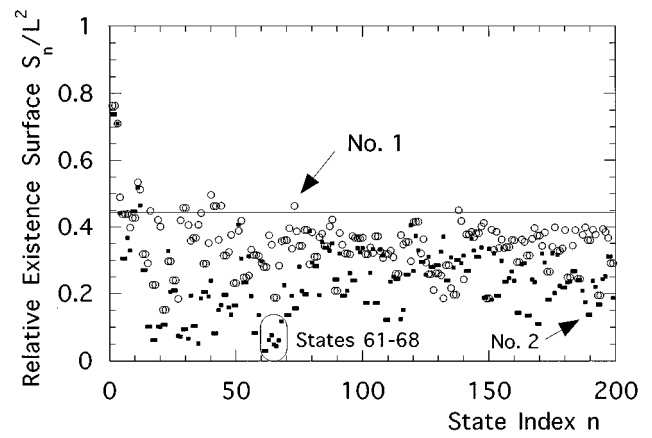


FIG. 4. Relative existence surface S_n/L^2 for the modes ($n \neq 0, m=0$). The localization surface decreases with the fractal generation. Some modes are strongly localized, e.g., modes 61–68 of cavity No. 2. The horizontal line at $S_n/L^2=4/9$ corresponds to the modes of the square.

resonators being small. To characterize mathematically the localization or the confinement of each mode Ψ_n , we compute the “existence surface” S_n defined by Thouless as²⁰

$$S_n = \left[\int dx dy |\Psi_n|^4 \right]^{-1}. \quad (13)$$

If we find that S_n is significantly smaller than the surface L^2 of the cross section, we say that this particular mode is “localized.” Note that for the delocalized cosine functions of the square system, the value of the relative occupation surface is $S_n/L^2=4/9 \approx 0.44$ for all modes.

The values of the relative existence surface S_n/L^2 for our geometries are shown in Fig. 4. Apart from the very first states, the existence surface is only a fraction of the total surface of the resonator. Most important, the tendency to localization is increased by the irregularity of the frontier. For generation 1 the average $\langle S_n/L^2 \rangle$ over the first 200 lower states was found to be equal to 0.35. For generation 2, the average $\langle S_n/L^2 \rangle$ over the 200 states that we have computed is equal to 0.24. The highest degree of localization for this system is equal to 0.031 for the degenerated modes $n=61,62$. One should note that our systems have a rotation degeneracy which has the effect of increasing the existence volume. Without any symmetry the localization surface would be approximately four times smaller.

In Fig. 5 we show the amplitude distribution of a delocalized ($n=4$) and of a localized mode ($n=16$). The spatial location of confined modes is linked to the Neumann boundary condition for which the boundary region is free to vibrate. Eigenmodes can then have a maximum amplitude at the boundary. The confinement is a weak localization effect which does not occur for all states. When the fractal character of the frontier increases, i.e., from one prefractal generation to the next, we find more and more of these localized states. This is an important property of the Neumann modes.¹² Qualitatively, the more irregular and winding the boundary, the more localized the Neumann fractinos. We expect a similar behavior for systems which are irregular in the three spatial directions.

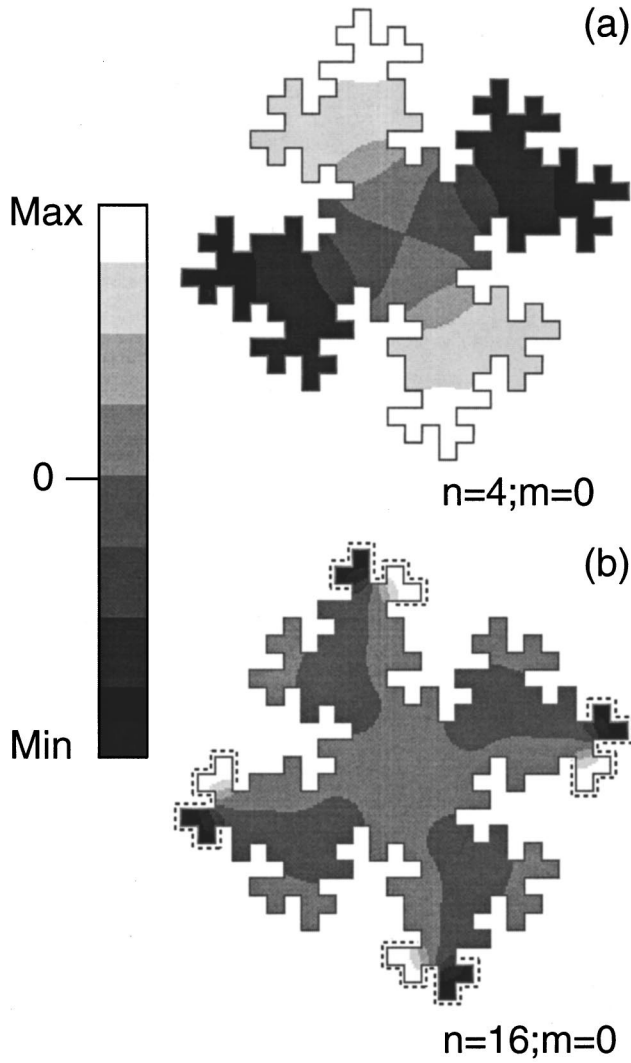


FIG. 5. Two particular modes of the prefractal cavity No. 2. (a) Mode $n = 4$, $m = 0$; (b) mode $n = 16$, $m = 0$. The amplitudes are indicated by different gray levels. Black and white regions stand for extremum positive and negative pressures. The gray tones stand for low pressures. Mode (a) is an example of delocalized state, while mode (b) is an example of localized state. Localization occurs at the cavity boundary. The dashed line indicates the perimeter L_p of the zone where the mode is confined. It is also the region where the energy is dissipated.

The effect of localization is to enhance locally the amplitude of the vibration at the cavity walls in the region where the energy is dissipated. There exists a correlative increase of the integral in Eq. (12). If, in a very crude approximation, one considers the mode as constant over its existence surface and zero outside, its amplitude is of order $S_n^{-1/2}$. Integral (12) gives a value

$$\Lambda_N^{-1} \cong S_n^{-1} L_p, \quad (14)$$

where L_p is the *perimeter* of the zone where the states really exist.

Consider for instance mode $n = 16$, shown in Fig. 5(b). Its existence volume is approximately given by the surface of the black and white regions: $S_n \cong 4 \times 8 (L/16)^2 = L^2/8$. The perimeter of the zone where the amplitude is large, as indicated by the dashed contour in the figure, is of order $L_0 \cong 4 \times 15 (L/16)$ and from Eq. (14) $L/\Lambda_N \cong 30$. For this mode the

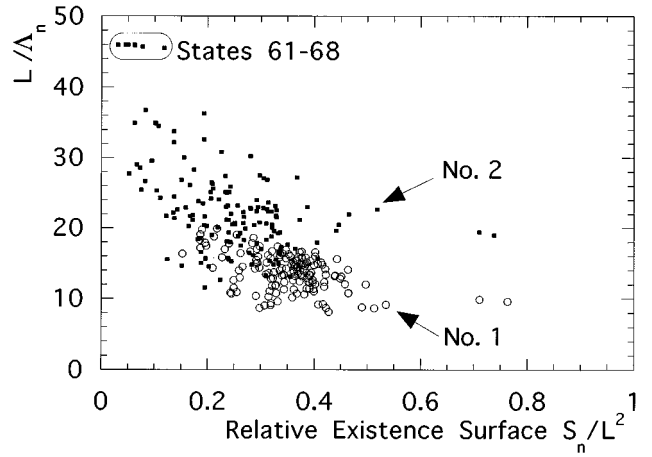


FIG. 6. Dissipation versus localization. The losses increase from one prefractal generation to the next, while the localization volume decreases. States 61–68 of cavity No. 2 which are strongly localized have the largest losses.

numerical value is $L/\Lambda_N = 35$, in good agreement with our crude approximation. This approximation also applies to the strongly localized states 61–68 of system No. 2. These states, which are discussed in Ref. 12, have the highest losses.

The power dissipation as a function of the relative existence surface is shown in Fig. 6. In spite of a strong dispersion, the global trend is indeed an increase of the losses with irregularity and localization.

Equation (14) is of extreme importance because it shows that for a given localized mode, if one locally increases the perimeter, the losses are increased correspondingly. It means that a mathematical fractal would also exhibit infinite damping for these higher-order modes (with the same restrictions than above).

The quality factor for a mode N can be written in our reduced units:

$$Q_N = \pi(\Omega_N \Lambda_N / L) / [\text{Re } \epsilon(\omega_N)]. \quad (15)$$

We have plotted in Fig. 7 the numerical values of the factor

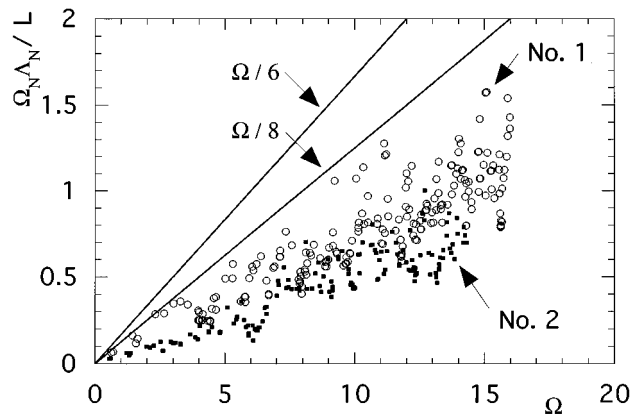


FIG. 7. Quality factor, measured by $\Omega_N \Lambda_N / L$, of the low-frequency modes with $m = 0$ as a function of the reduced frequency Ω . For the cube the values of $\Omega_N \Lambda_N / L$ are equal to $\Omega_N / 6$ for the modes $\mu = 0$, $\mu' \neq 0$ (or $\mu \neq 0$, $\mu' = 0$) and are equal to $\Omega_N / 8$ if $\mu \neq 0$, $\mu' \neq 0$. This is indicated by the two lines. The higher the geometrical irregularity, the lower the quality factors.

$\Omega_N \Lambda_N / L$ as a function of the reduced frequency Ω_N for our three cavities. One observes that for all frequencies the irregular cavities present lower quality factors than the cube. Despite the dispersion, increasing the irregularity induces a diminution of the quality factor.

VI. CONCLUSION

We have studied numerically the modal density, the localization, and the losses of acoustical modes in cavities with prefractal shapes. The modal density is enhanced by the irregularity of the boundary. Consequently, the level spacing decreases and becomes more regular. Acoustical losses have been studied in a boundary layer model and have been found to increase with irregularity. As far as our simplified model still applies, a mathematical fractal cavity would present an infinite damping. We have established a simple correspondence between localization and losses. These results confirm in a well-established physical frame the suggestion that fractal resonators present specific damping properties. Note that self-affine geometries¹ could even be more efficient than self-similar geometries in increasing the resonator perimeter, therefore the damping.

The same physical effects should appear in the propagation of sound waves in acoustical waveguides. Neglecting the anisotropy effects, the attenuation length for the acoustic energy of a propagating wave is of order $\Lambda_N / \text{Re}(\epsilon)$. Therefore, the data in Fig. 3 can be used to estimate the attenuation in fractal waveguides. Because of the localization, it should be possible to propagate higher-order localized modes in different regions of such an irregular waveguide with a small interference between these modes. Some of these effects could also exist in electromagnetic waveguides.

Further studies are needed to understand the influence of fractal geometry on ray acoustics which corresponds to the high-frequency limit of our problem.

Several of these results may be of interest for room acoustics. An increased low-frequency modal density could be favorable. On the other hand, localization may have negative consequences. Although our results on damping were obtained in the weak losses case, they can be considered a rationale to better understand the dependence of properties of anechoic chambers on geometry.

ACKNOWLEDGMENTS

One of us (SR) has benefited from the E. E. C. program ‘‘Human Capital and Mobility.’’ The computation was per-

formed at the ‘‘Institut du développement et des ressources en informatique scientifique’’ (IDRIS) in Orsay, France.

- ¹B. B. Mandelbrot, *The Fractal Geometry of Nature* (Freeman, San Francisco, 1982).
- ²B. Sapoval, *Fractals* (Aditech, Paris, 1990); *Universalités et Fractales* (Flammarion, Paris, 1997).
- ³B. Sapoval, ‘‘General formulation of Laplacian transfer across irregular surfaces,’’ *Phys. Rev. Lett.* **73**, 3314–3316 (1994).
- ⁴S. Russ and B. Sapoval, ‘‘Anomalous viscous damping of vibrations of fractal percolation clusters,’’ *Phys. Rev. Lett.* **73**, 1570–1573 (1994). For a review on fractons, see T. Nayama, K. Yakubo, and R. Orbach, ‘‘Dynamical properties of fractal networks: scaling, numerical simulations, and physical realizations,’’ *Rev. Mod. Phys.* **66**, 381–443 (1994).
- ⁵M. V. Berry, ‘‘Distribution of modes in fractal resonators,’’ in *Structural Stability in Physics*, edited by W. Guttinger and H. Elkeimer (Springer-Verlag, Berlin, 1979), pp. 51–53.
- ⁶M. L. Lapidus, ‘‘Fractal drum, inverse spectral problems for elliptic operators and a partial resolution of the Weyl-Berry conjecture,’’ *Trans. Am. Math. Soc.* **325**, 465–529 (1991), and references therein.
- ⁷J. Brossard and R. Carmona, ‘‘Can one hear the dimension of a fractal,’’ *Commun. Math. Phys.* **104**, 103–122 (1986).
- ⁸M. L. Lapidus and C. Pomerance, ‘‘The Riemann zeta-function and the one dimensional Weyl-Berry conjecture for fractal drums,’’ *Proc. London Math. Soc.* **3**, 41–69 (1993).
- ⁹J. Fleckinger, M. Levitin, and D. Vassiliev, ‘‘Heat equation on the triadic von Koch snowflake: Asymptotic and numerical analysis,’’ *Proc. London Math. Soc.* **71**, 372–396 (1995).
- ¹⁰B. Sapoval and Th. Gobron, ‘‘Vibrations of strongly irregular or fractal resonators,’’ *Phys. Rev. E* **47**, 3013–3024 (1993).
- ¹¹B. Sapoval, Th. Gobron, and A. Margolina, ‘‘Vibrations of fractal drums,’’ *Phys. Rev. Lett.* **67**, 2974–2977 (1991).
- ¹²S. Russ, B. Sapoval, and O. Haerberlé, *Phys. Rev. E* **55**, 1413 (1997).
- ¹³Y. Hobiki, K. Yakubo, and T. Nakayama, ‘‘Spectral characteristics in resonators with fractal boundaries,’’ *Phys. Rev. E* **54**, 1997–2004 (1996).
- ¹⁴P. M. Morse and K. Uno Ingard, *Theoretical Acoustics* (Princeton U. P., Princeton, 1968).
- ¹⁵A. D. Pierce, *Acoustics: An Introduction to Its Physical Principles and Applications* (McGraw Hill, New York, 1981).
- ¹⁶M. Bruneau, *Introduction aux théories de l’acoustique* (Université du Maine éditeur, Le Mans, 1983).
- ¹⁷M. Bruneau, C. Garing, and H. Leblond, ‘‘Quality factor and boundary-layer attenuation of low order modes in acoustic cavities,’’ *J. Phys. (Paris)* **46**, 1079–1085 (1985).
- ¹⁸D. L. Koch, ‘‘Attenuation of compressional sound waves in the presence of a fractal boundary,’’ *Phys. Fluids* **30**, 2922–2927 (1987).
- ¹⁹H. P. Baltes and E. R. Hilf, *Spectra of Finite Systems* (BI Wissenschaftsverlag, Vienna, 1976).
- ²⁰D. J. Thouless, ‘‘Electrons in disordered systems and the theory of localization,’’ *Phys. Rep.* **13**, 93–142 (1974).